JOURNAL OF MATERIALS SCIENCE 27 (1992) 2193–2198

Mechanical properties and fracture characteristics of aged Cu–1.8 wt% Be–0.2 wt% Co alloy in various loading modes

Y. ROSENTHAL
Nuclear Research Center—Negev, PO Box 9001, Beer Sheva 84190, Israel

The fracture of a Cu–Be alloy was examined in various loading modes. For the tensile mode, two degrees of ageing were also tested. The common fracture mode was defined as a dimpled intergranular, and its relation to the precipitate morphology is discussed.

1. Introduction

The extensive use of wrought Cu–1.8 wt% Be–0.2 wt% Co alloys in electronics, instrumentation and cryogenic technology is due to their outstanding physical and mechanical properties. These alloys lend themselves to a variety of heat treatments, resulting in a remarkable combination of high electrical and thermal conductivity, very low magnetic permeability, moderate Young modulus and high elastic limit, dimensional stability, mechanical strength comparable to that of the best machinery steels (and almost always in the temperature range from −80 to 200 °C), and lack of creep or relaxation under normal service stresses and temperature up to 90 °C. Considerable efforts have been dedicated towards understanding the unloading and yield point effects [1, 2], dynamic strain ageing [3], precipitation mechanisms [4–7], and precipitation hardening [8–12] in these alloys.

No information, however, is available on the fracture characteristics of this alloy. The main purpose of the present work is to study the fracture of this alloy in various loading modes, and to understand it as the final event of certain thermomechanical histories.

2. Experimental procedure

The alloy investigated was a commercial copper–beryllium alloy in the form of sheets, round bars and thick plates with a nominal composition of 1.8 wt% Be–0.2 wt% Co. A supersaturated solid solution was obtained by solution-treating the material at 800 °C for 1 h followed by water quenching. The material was subsequently aged at 315 °C for 3 h. This temper was chosen since it represents roughly the average degree of work hardening achieved in a variety of industrial drawing processes. Two additional ageing treatments at 180 and 240 °C for 1 h were also applied to one of the sheet materials for comparison. The degree of ageing was evaluated by low-load (Vickers) hardness testing, using an optical Finotest (Frank) hardness tester, giving a value of 420 Hv (150 and 180 Hv for the 180 and 240 °C ageing treatments, respectively).

Various mechanical test methods and loading modes were used. Flat (0.5-mm-thick) and round (5.6-mm gauge diameter) tensile specimens were prepared according to the ASTM E-8 test method. Tensile testing, as well as data acquisition and analysis, was performed on an on-line computerized system based on an Instron machine and a personal computer [13].

Charpy specimens were prepared according to the ASTM E-24 test method. Fatigue precracking was performed on some of the specimens according to ASTM E-399 test method using a Manlabs FCM-3000 precracker (NRCN (TN) report, to be published). The specimens were fractured in an on-line computerized instrumented impact system based on a Tinius Olsen impact machine and a mini-computer [14].

Standard chevron-notched three-point bend specimens were prepared from the thick plate. These specimens do not require specialist machining or testing capabilities, and are potentially inexpensive, largely due to the absence of a fatigue precrack. Fracture mechanics tests conforming to the ASTM test method for plane-strain fracture toughness of metallic materials (E-399) were performed in bending on the tensile testing system described above.

Three-point bend specimens were fatigue precracked in a Rumul Cracktronic resonance precracker and tested in a MTS servo hydrolic machine conforming to the ASTM E-399 test method. The fracture surfaces of the various mechanical testing specimens were examined after the tests using a Phillips scanning electron microscope (SEM) operating at 15 kV.

3. Results and discussion

The tensile data are summarized in Table I. Engineering stress–strain curves of the flat and round specimens are shown in Fig. 1.

Comparisons are drawn between the mechanical properties and the fracture appearance of the alloys in the "fully aged" (both flat and round specimens aged at 315 °C) and in the 'half hard' (flat specimens aged at

0022–2461

TABLE I Mechanical properties in tension of Cu–1.8 wt % Be–0.2 wt % Co at various ageing conditions and specimen geometries. The averages shown are based on five specimens per condition.

Specimen	Yield stress (MPa)	UTS		Fracture stress	
		Stress (MPa)	Strain (%)	Stress (MPa)	Strain (%)
Flat, fully aged	1185	1285	3.2	1285	3.2
Flat, aged at 240 °C	578	770	22.5	705	27.7
Flat, aged at 180 °C	320	535	30.1	470	31.8
Round, fully aged	1282	1415	3.7	1363	8.9

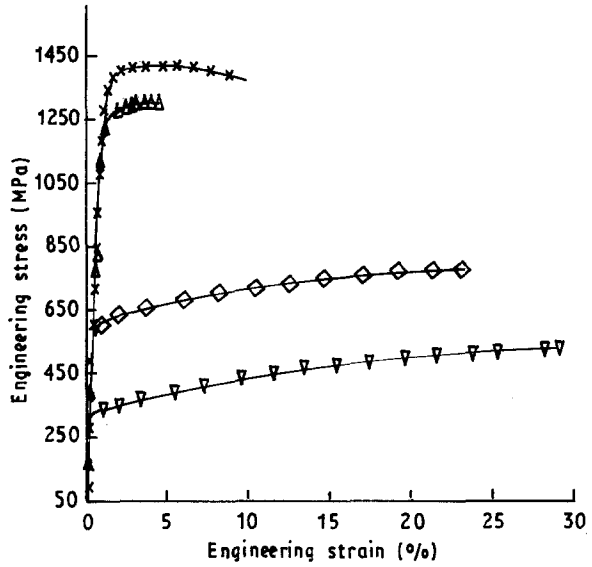

Figure 1 Engineering stress–strain curves. Round specimens: (×) 5.6 mm, aged at 315 °C. Flat specimens: 0.5 mm, aged at (△) 315; (◇) 240; (▽) 180 °C.

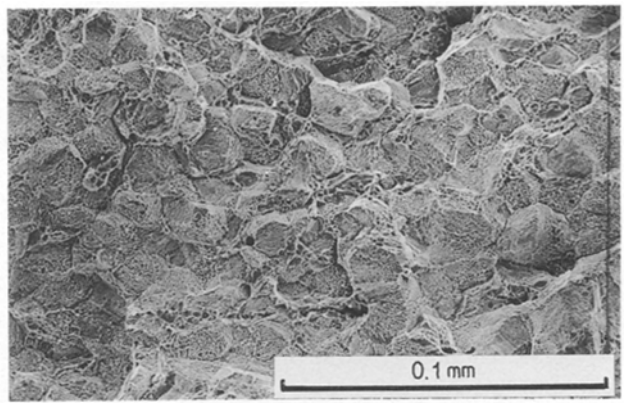

Figure 2 Fracture of a flat fully-aged tensile specimen.

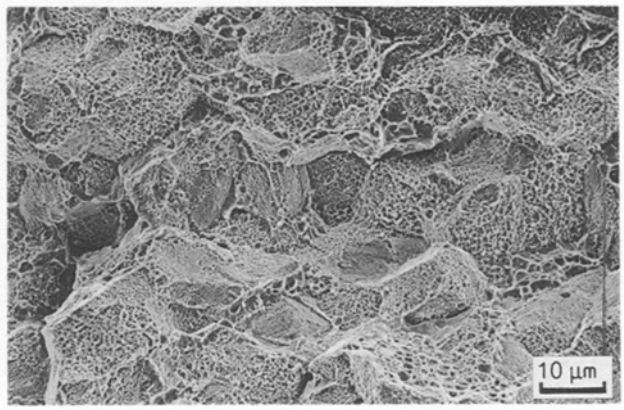

Figure 3 Fracture of a flat half-aged tensile specimen.

180 and 240 °C) conditions. Geometry effects are assumed to be the reason for the higher stress level of the tensile round specimens, in comparison to the tensile flat specimens. These effects are also related to the apparent difference between the uniform elongation, e_u, and the elongation to fracture, e_f, which appeared only in the tensile round specimens.

Fractographs taken from the fracture surfaces of fully aged flat (Fig. 2) and round specimens show a transgranular mode with void coalescence on grain-boundary facets. The mechanical properties and the fracture appearance of the half hard flat specimens, as seen in Table 1 and Fig. 3, differ from the above results. The stress level is lowered by about 50% (240 °C ageing) and 67% (180 °C) and the alloy is much more ductile (e_u = 30%). However, the fracture mode in these specimens is also dimpled transgranular, typical of ductile fracture.

The load–time curves obtained during the instrumented impact tests are shown in Fig. 4. Load–time data of precracked charpy specimens was used to obtain the dynamic stress-intensity factor coefficient, K_{Id} [15], resulting in a value of 51 MPa $m^{1/2}$. A fractograph of the fracture surface of the impacted specimen is presented in Fig. 5. Similarly to the aged tensile specimens, a transgranular fracture path with deeper dimples on grains can be observed. The surface

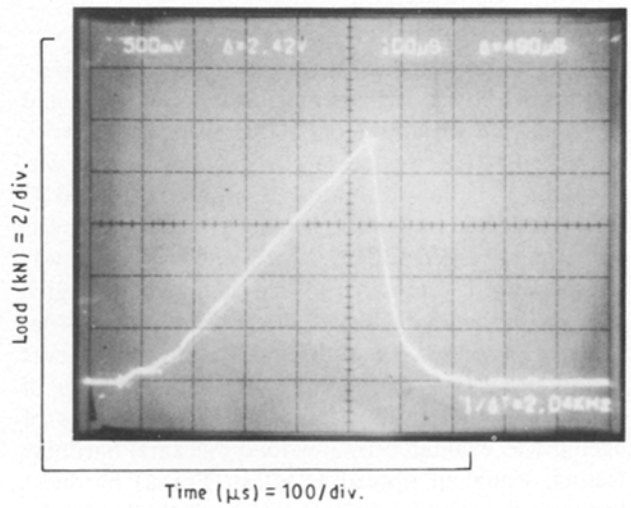

Figure 4 Load–time curve obtained in an instrumented impact test.

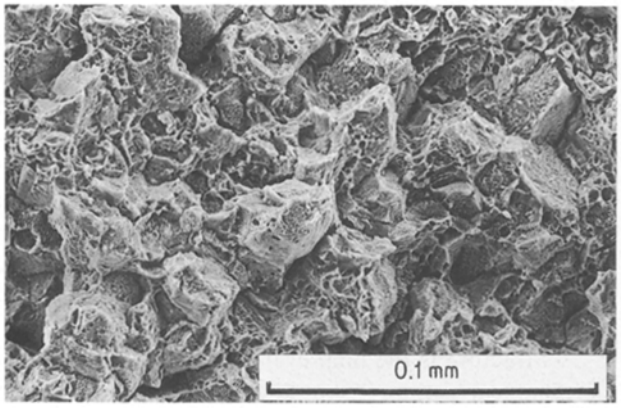

Figure 5 Fracture appearance of the precracked charpy specimen.

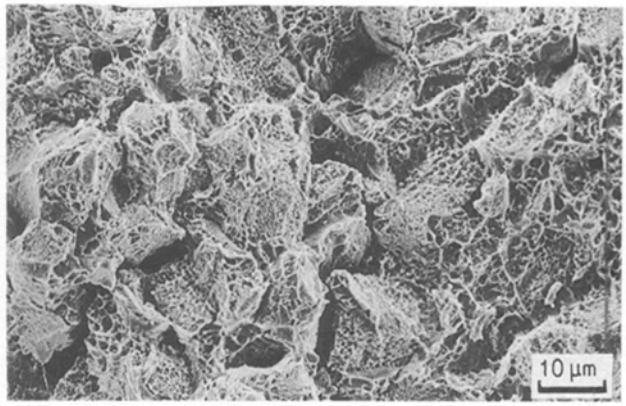

Figure 7 Fracture surface of the charpy specimen, ahead of the fatigue crack front.

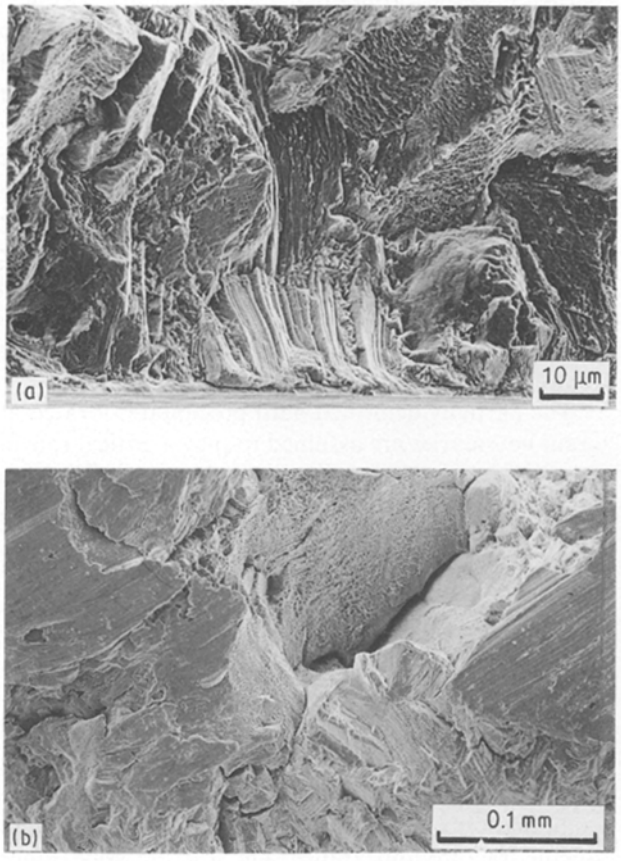

Figure 6 (a) Micro- and macrocleavage near the starter notch in the fatigue crack surface. (b) Same area as in (a) showing that microcleavage occurred at twisted-boundary grains.

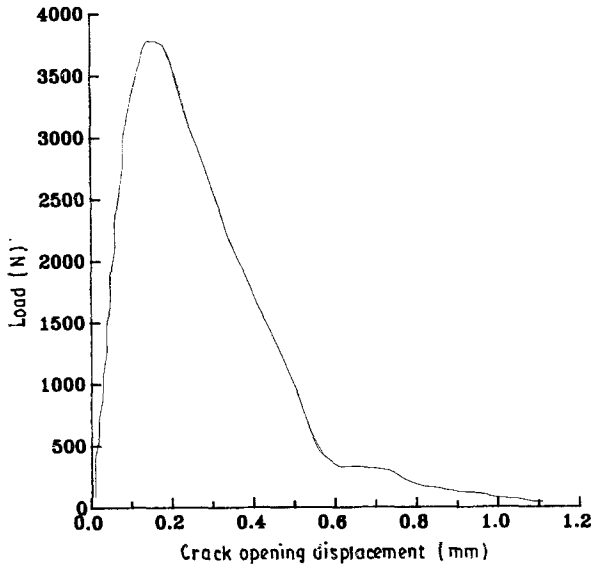

Figure 8 Load–displacement curve of a chevron-notched three-point bend specimen.

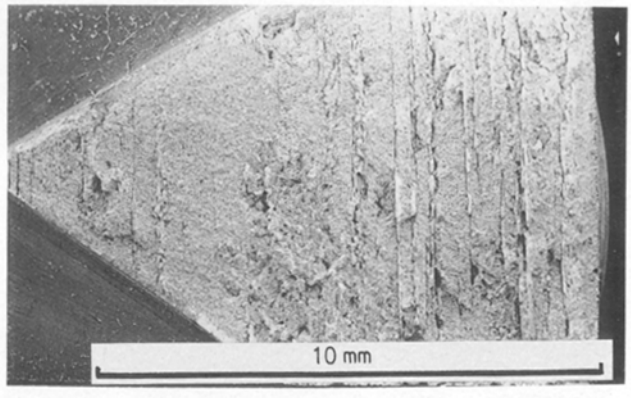

Figure 9 Overall view of the fracture surface in the chevron-notched specimen.

of the fatigue precrack, grown in an impact specimen, is shown in Fig. 6, and the area of the final fracture is shown in Fig. 7. The fatigue crack surface, near the starter notch, reveals micro- and macro-cleavage modes (Fig. 6a). A discontinuous 'river' pattern across some of the grains also appears, suggesting that microcleavage occurs at grains (Fig. 6b) connected by a twist boundary. Microvoid coalescence on cleaved grains starts to appear as the fatigue crack propagates through the fine final growth area. However, the fracture surface ahead of fatigue crack front shown in Fig. 7 is associated with a dimpled intergranular mode originating from void coalescence along grain boundaries. A typical load–displacement curve, obtained during the test with a chevron-notched bend specimen, is shown in Fig. 8: K_{Ic}, as calculated for a chevron-notched bend specimen [16], was 48.3 MPa $m^{1/2}$.

An overall view of the fracture face is shown in Fig. 9. Two readily distinguishable fracture zones are apparent: a stable crack growth zone developed at the

chevron tip, and an unstable crack growth zone developed when the crack length reaches a critical value. The first zone is characterized mostly by intergranular fracture with shallow dimples on grain boundaries (Fig. 10). A few deep cracks, perpendicular to the failure direction, are also visible in this zone, some of which are composed of cleaved grains (Fig. 11). The fracture appearance in the unstable crack-growth zone is different where a large number of the deep perpendicular cracks can be observed (Fig. 12). The unstable crack propagates in a quasi-cleavage mode, thus creating deep cracks across the chevron section separated by dimpled intergranular rapture areas between the cracks. These transverse cracks suggest that "jumping" occurred during the unstable crack propagation, although no load drops were visible in the load–COD curve (Fig. 8).

Data analysis of the fracture toughness plane-strain tests resulted in a stress intensity factor coefficient K_{Ic} value of 34 MPa $m^{1/2}$. The fracture surface reveals the precrack surface, grown from the starter notch in fatigue, and the final failure surface. Transgranular fracture with cleaved grains (Fig. 13) is the dominant fracture mode at the beginning of the fatigue precracking, near the starter notch. River marking (striations) appears (Fig. 14) as the crack moves along a number of parallel planes, which form a series of plateaux and connecting edges. The pre-observed dimpled intergranular rapture was also observed through the section of the final fracture surface.

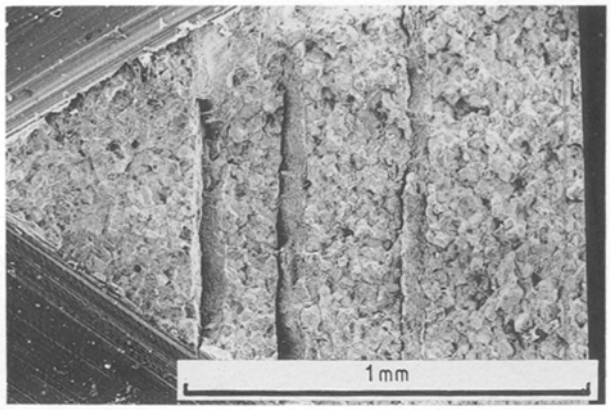

Figure 10 Stable crack growth near the chevron tip.

Interpretation of the various tests suggests that the fracture appearance depends on the test mode and applied loading rate. Tensile failure of smooth tensile specimens can generally be characterized as dimpled transgranular, independent of heat treatment. Loading of notched and precracked specimens resulted in dimpled intergranular failure, the dimple size and distribution depending upon the loading rate. However, these fracture modes were altered when fatigue precracking was involved: here, brittle cleavage was observed.

As fracture is the final event in a complex thermomechanical history, it should represent the interaction between the state of the applied stress in the mechanical testing and the microstructure. The influence of ageing processes (precipitation hardening) on the strengthening of Cu–Be–Co alloys has been found in earlier research programmes, mostly using hardness testing [4, 7–9, 12, 17, 18]. In some of these works the microstructure was characterized using SEM and TEM, and it was suggested that the mechanism of participation follows the sequence of supersaturated solid solution > GP zones > τ' phase > τ phase (no transformation of τ' to τ was observed up to 320 °C) [5, 6, 10, 11, 19, 20]. It was concluded that the sequence of continuous and discontinuous (depending strongly on the ageing temperature below 380 °C) precipitation nucleated at grain boundaries and growing into the adjoining grains is the result of the ageing treatment tested in this study.

The partially deformed hard precipitates located at grain boundaries are assumed to play a critical role in the high-strength low-ductility material, the fracture mode of which is defined as dimpled intergranular. Gadalla [21] came to similar conclusions using SEM and TEM examination of tensiled specimens. SEM observations, in this study, revealed the failure path along grain boundaries covered with small, shallow dimples. It is therefore assumed that the shear deformation of discontinuous precipitates at grain boundaries contributes to the minimal ductility of the aged alloy. The half-hard condition, however, is associated with incomplete transformation, which yields the combination of moderate strength and ductility and ductile fracture appearance. The fracture appearance of fatigue precracked areas is different. The surface is

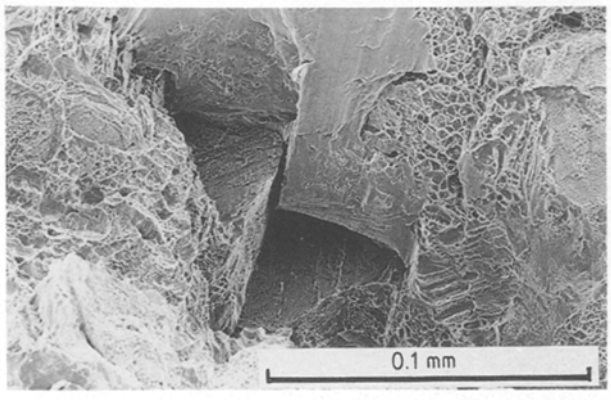

Figure 11 Cracks, perpendicular to the failure direction, in the stable growth zone.

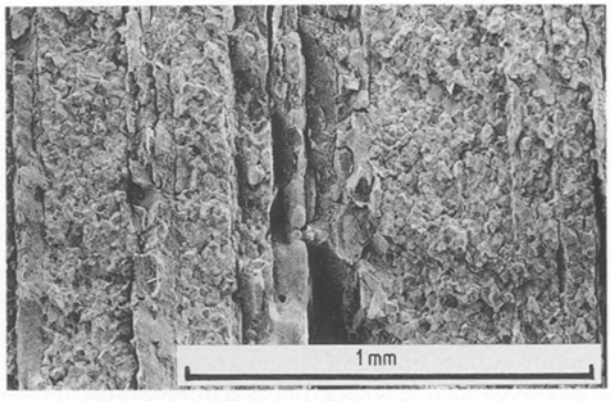

Figure 12 Large number of deep perpendicular cracks, composed of cleaved grains, and separated by intergranular ruptured grains.

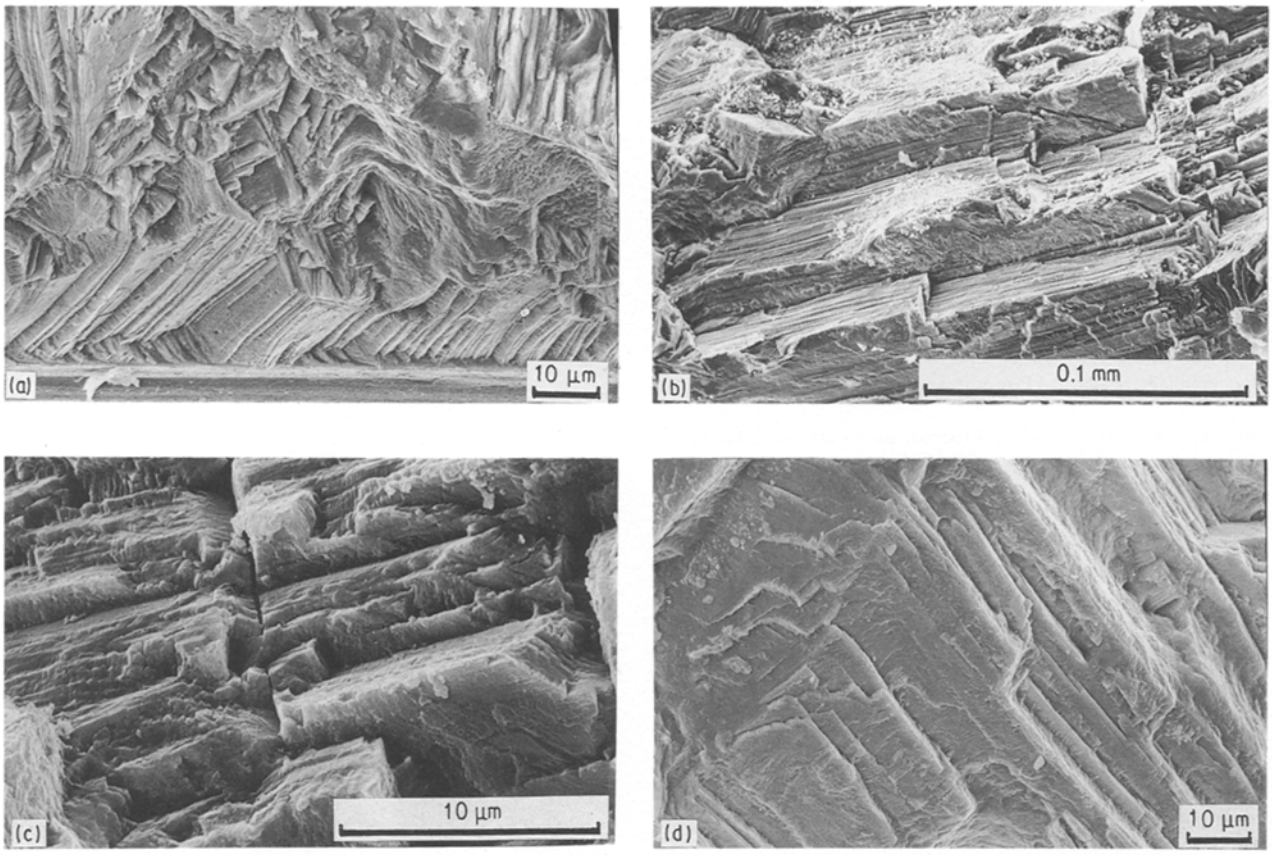

Figure 13 (a) Starter notch (at the bottom) and beginning of the fatigue precrack in a fracture throughness bend specimen. (b) Same specimen as in (a): brittle cubic cleaved grains are apparent when the crack develops further. (c) As the crack advances, massive cleavage is the dominant mode associated with transverse cracks. (d) The final "fine" crack-growth surface reveals a similar structure, although the cracks are shallower.

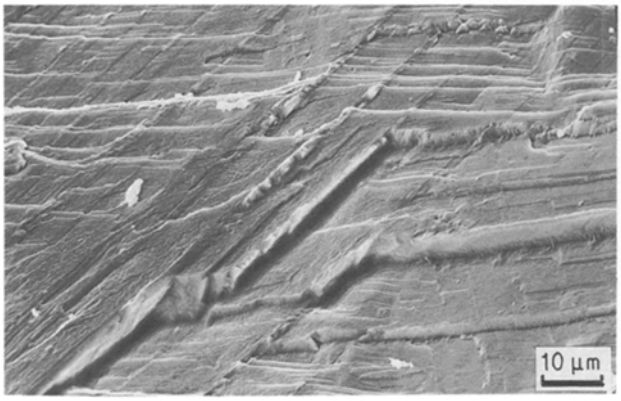

Figure 14 Striations in the cracked surface of a fracture throughness bend specimen.

deformed by cyclic slip, concentrated in persistent slip bands with irregular notched profiles consisting of extrusions and intrusions which eventually form cracks along slip planes. This slip-plane cracking is extended for a few grain diameters near the starter notch, and then changes to a continuum mechanism of crack propagation.

The cracks in the case of the chevron bend specimens, perpendicular to the direction of the applied stress, need more explanation. Gadala [21] has also shown that Cu–Be alloy is a low-stack alloy, as indicated by the existence of deformation twins and by the dislocation structure (due to the low-stacking-fault energy, dislocations in the deformed specimens did not form the cell structure, but formed a structure similar to the Ag– and Cu–Zn alloys). In his work [21], cracks were initiated and propagated along grain boundaries, with the general direction of crack propagation coinciding with the plane perpendicular to the direction of the applied stress. Work is now under way to try to explain why this phenomenon was found only in this type of specimens, and to explore the influence of this mode of crack propagation on the fracture mechanics parameters.

Acknowledgements

The author is indebted to Avi Magen, Ofer Sabag, Moshe Cohen, Zvi Hagag and Maymon Cohen for their assistance in mechanical testing, to Z. Barkai and S. Zalkind for the electron microscopy, and to A. Bossiba for the fracture mechanics tests.

References

1. G. F. BOLLING, *Phil. Mag.* **4** (1959) 537.
2. A. T. THOMAS, *ibid.* **5** (1960) 947.
3. R. B. JONES and V.A. PHILIPS, *Trans. ASM* **53** (1960) 603.
4. B. DJURIC and M. JOVANOVIC, *Metallography* **13** (1980) 235.
5. R. J. RIOJA and D. E. LAUGHLIN, *Acta Metall.* **28** (1980) 1301.
6. P. WILKES and M. M. JACKSON, *Met. Sci. J.* **3** (1969) 130.
7. A. R. ENTWISLE and J. K. WYNN, *J. Inst. Metals* **89** (1960/61) 24.

8. P. A. BECK, *J. Appl. Phys.* **20** (1949) 666.
9. F. SACHSLEHNER, V. GROGER and F. STANGLER, *Met. Sci.* **18** (1984) 153.
10. W. BONFIELD and B. C. EDWARDS, *J. Mater. Sci.* **9** (1974) 398.
11. *Idem. ibid.* **9** (1974) 409.
12. *Idem. ibid.* **9** (1974) 415.
13. G. ADAM, Y. A. ROSENTHAL and G. KOHN, *Intell. Instr. Comp.* **61** (1988) 13.
14. M. M. MARKOVITCH, Y. ROSENTHAL and G. ADAM, *J. Test. Eval.* **15** (1987) 265.
15. D. R. IRELAND, in Proceedings of the CSNI Specialist Meeting No. 67 on Instrumented Charpy Testing, Palo Alto, November 1981, EPRI report NP-2102-LD, edited by R. A. Wullaert (Electrical Power Research Institute, Palo Alto, 1981) p. 1.
16. W. SHANG-XIAM, in Proceedings of the Symposium on Chevron Notched Specimens: Testing and Stress Analysis, STP-855, Louisville, April 1983, edited by J. H. Underwood, S. W. Freiman and F. I. Baratta (ASTM, Philadelphia, 1983) p. 176.
17. H. KREYE, *Z. Metallkde.* **62** (1971) 556.
18. M. MARKOVITCH, P. COHEN, R. FRENKEL, S. NAHMIAS and E. POLLAK, in Research Laboratories Annual Report, January-December 1971, report IA-1262 (Israel Atomic Energy Commission, 1972) p. 58.
19. Y. MISHIMA and R. SHIROMIZU, *Trans. Metall. Soc. AIME* **242** (1968) 751.
20. M. NAKAGAWA, *Jpn. J. Appl. Phys.* **4** (1965) 760.
21. A. A. GADALLA, *Ind. J. Pure Appl. Phys.* **18** (1980) 307.

Received 4 January
and accepted 7 June 1991